

process overlooks the diversity of multi-modal trajectories. (ii) The standard ADE and FDE metrics do not consider any type of prediction confidence such as a probability or rank of each trajectory. In practice, however, such a confidence factor should be provided and evaluated in applications where the ground-truth is not available during inference. Considering these limitations, we additionally introduce new error metrics based on ADE and FDE to properly evaluate the diversity of multi-modal predictions with their associated confidence.

II. RELATED WORKS

A. Deep Learning on Trajectory Forecast

Deep neural networks have been used with great success in modeling interactions between humans in a data-driven manner. A recurrent neural network (RNN) has been widely used to encode the history of pedestrians' motion [6], [1], [2], [15], [16]. RNNs use a pooling mechanism to extract interaction information by aggregating the encoded motion features of different individuals. However, such hand-crafted or arbitrary aggregation methods may hinder the acquisition of important representations for future trajectory generation. To address this limitation, a graph neural network has been introduced in this domain. The inherent node-edge topology of graphs helps to model more intuitive and natural interactions between humans [3], [17], [13], [7]. Rather than pooling the information, these approaches find interactions between agents, corresponding to updating edges. However, they are prone to error accumulation over the time horizon because of their structural dependency on recurrent units [3], [17], limited in modeling interactions in space and in time [13], or do not properly capture the importance of interactions in a spatio-temporal space [7]. In contrast, our aim in this work is to propose an approach that can overcome such limitations using graph neural networks [18] with multi-attention in space and in time.

B. Multi-Modal Trajectory Forecast

The importance of multi-modality in trajectory prediction has become more widely recognized in recent years. Considering that multiple plausible trajectories may exist with the given information, some works [6], [3], [7], [5] generate a bi-variate Gaussian distribution and sequentially sample the pedestrian's future locations. Other works address the multi-modality of the future prediction using mixture models [19], [20], [21], [8], [9], [4]. However, their predictions tend to be a single mode with high variances [10]. There are also methods that extend deep generative models to learn the distribution of future trajectories over data. These methods use either variational autoencoders (VAEs) [1], [11], [12] or generative adversarial networks (GANs) [2], [22]. Although they are expected to generate multi-modal human behavior, such random sampling-based strategies are prone to experiencing problems with mode collapse [7] or posterior collapse [12]. More importantly, those works do not measure the probability of individual modes, and therefore, their multi-modal predictions have practical limitations in many real applications. [23] recently addresses more practical

functionality of multi-modality by providing the probability of each trajectory output. However, a predefined trajectory set is used to represent the different modes of future motion, which is difficult to generalize across different environment types. In this work, our model not only generates interaction-specific multi-modal future trajectories with diversity, it also outputs probabilities associated with individual modes.

C. Evaluation Metrics for Trajectory Forecast

Evaluation of future trajectory has been conducted by computing Euclidean (L_2) distance between the predicted and ground-truth locations at every future time step. The error is reported by measuring the average distance error (ADE) during a specified time interval, and the final distance error (FDE) at a specified time. Since these metrics are intuitive and directly quantify the performance of prediction algorithms, they are generally used in evaluation of performance in previous approaches [6], [3]. For multi-modal evaluation, [1] simply extends the same metrics in an oracle manner by evaluating one with the lowest error. Their method computes the performance upper bound instead of evaluating the diversity or plausibility of multiple modes. [24], [25] introduce the kernel density estimate-based negative log-likelihood (KDE_NLL) metric that computes the log-likelihood of the ground-truth against the sampled trajectory distribution. The KDE function often underestimates the output distribution, approximating as a Gaussian kernel. When multiple trajectory modes are predicted (e.g., different trajectories at an intersection), it does not properly capture the multi-modality because of the kernel approximation. In contrast, the proposed metrics avoid this potential problem without the approximation and directly evaluate the diversity of multi-modal trajectories with associated probabilities.

III. METHODOLOGY

A. Problem Formulation

Given a scenario with K agents and their motion information, we use the first T_{in} time steps of trajectories $X = \{X^1, X^2, \dots, X^K\}$ to predict the next T_{out} time steps of trajectories $Y = \{Y^1, Y^2, \dots, Y^K\}$. We denote $X^k = \{x_t^k | \forall t \in \{1, \dots, T_{in}\}\}$ and $Y^k = \{y_t^k | \forall t \in \{1, \dots, T_{out}\}\}$ for each agent $k \in \{1, \dots, K\}$. x_t^k and y_t^k can be further represented by 2D positions of agent k at time t . Our framework outputs M modes of future trajectories $\hat{Y}_m^k = \{\hat{y}_{(m)1}^k, \hat{y}_{(m)2}^k, \dots, \hat{y}_{(m)T_{out}}^k\}$ with their probabilities p_m^k for all K agents in the scene, where $m \in \{1, \dots, M\}$, such that $\sum_m p_m^k = 1$.

B. Spatio-Temporal Multi-Attention Graph Convolutions

We create a graph representation $G_t = (V_t, E_t)$ at each time step $t \in \{1, \dots, T_{in}\}$, where $V_t = \{v_t^k | \forall k \in \{1, \dots, K\}\}$ is a set of nodes and $E_t = \{e_t^{ij} | \forall i, j \in \{1, \dots, K\}\}$ is a set of edges. $v_t^k = x_t^k - x_{t-1}^k$ is a node attribute represented as a relative motion for agent k , which also encodes the heading at each time-step. Also, e_t^{ij} is an edge attribute where e_t^{ij} indicates the connectivity between two node attributes.

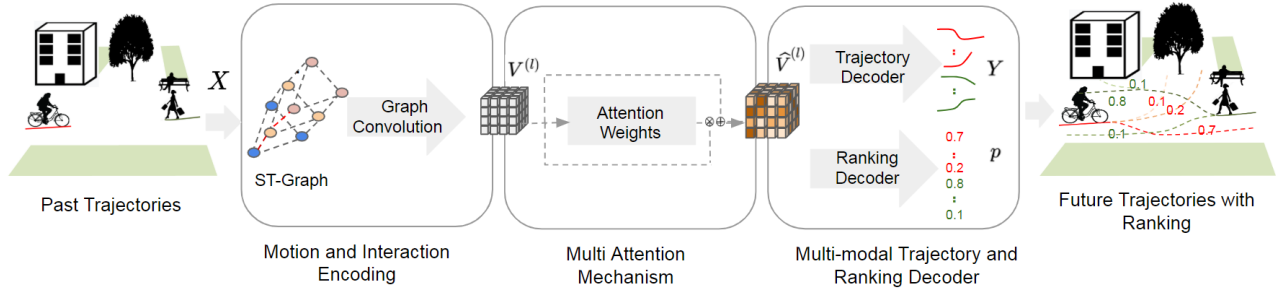


Fig. 2. Social-STAGE Framework: Given input scenario with agents’ (shown in different colors) past trajectories (shown in dotted line), we perform ST-Graph Convolutions and multi-attention mechanism for encoding meaningful interactions. The encoded features are decoded into multi-modal trajectories (for all agents) and corresponding probabilities to rank each mode. The opacity of each future trajectory prediction is changed to show the corresponding probability in the final output.

We follow the procedure as in [18], [14] for the implementation of graph convolutions. We define the adjacency matrix A_t where its element a_t^{ij} indicates the importance weight of the edge between two node attributes v_t^i and v_t^j . The weight is represented using a kernel function similar to [7], $a_t^{ij} = 1/\|v_t^i - v_t^j\|_2$ if $i \neq j$, otherwise $a_t^{ii} = 0$. To ease training, we adopt a renormalization trick. Therefore, the adjacency matrix is symmetrically normalized as

$$A_t = \lambda_t^{-1/2} \hat{A}_t \lambda_t^{-1/2} \quad (1)$$

where λ_t is a diagonal node degree matrix of A_t and $\hat{A}_t = A_t + I$ adds self-connections to A_t with an identity matrix I . For spatio-temporal extension, we stack the adjacency matrices $A = \{A_t | \forall t \in \{1, \dots, T_{in}\}\}$ and nodes $V = \{V_t | \forall t \in \{1, \dots, T_{in}\}\}$ for all observation time steps. In addition, \hat{A} is stack of \hat{A}_t and λ is stack of λ_t . Therefore, the node attributes $V^{(l)}$ of layer l are updated using the adjacency matrix as follows:

$$f(V^{(l)}, A) = \sigma(\lambda^{-1/2} \hat{A} \lambda^{-1/2} V^{(l)} \mathbf{W}^{(l)}), \quad (2)$$

where σ is an activation function and $\mathbf{W}^{(l)}$ is the trainable weights of layer l .

Therefore, the resulting node attributes are formulated as graph convolutional features for spatio-temporal interactions. We further use temporal convolutions and the softmax operation to obtain the attention weights. Such weights correspond to the relative importance of interactions, describing the time when the interaction should be captured and the agent who should be identified. We use the term multi-attention as individual agents can be simultaneously attentive along the spatial and temporal dimension. Note that this process is different with prior works [3], [17], where a single attentive weight is locally generated in space with a recurrent fashion. As a result, we can capture social interactions activated across different spatial and temporal locations. The multi-attention weights are updated by the residual connection similar to [26]. This leaves us with the following operation:

$$\hat{V}^{(l)} = (\phi(V^{(l)}) \otimes V^{(l)}) \oplus V^{(l)}, \quad (3)$$

where ϕ denotes a convolution operation to compute attention weights, \otimes denotes element-wise multiplication, and \oplus denotes element-wise sum operation. The updated features $\hat{V}^{(l)}$ are multi-attention features with attentive weights of

spatio-temporal interactions. This process is visualized in Figure 3, and the detailed network architecture is presented in the Section V.

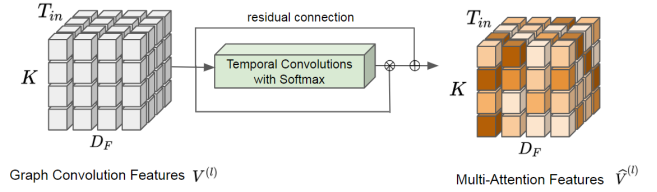


Fig. 3. Multi Attention: \oplus and \otimes are element-wise sum and multiplication respectively

C. Ranking and Decoding

To address the practical usage of multi-modality, we introduce probability measures for each output trajectory mode to rank the confidence in our predictions. This step is displayed in Figure 4. The first stream is constructed with temporal convolutions with a PRelu operation in the decoder to generate M future trajectories of K agents for T_{out} time steps. Therefore, each output trajectory matches to one of the modes. Since in our implementation the dimension of multi-attention features D_F is same as the dimension of the output trajectory D_{out} , no additional operations are necessary to match the dimensions. The second stream generates probabilities corresponding to individual output modes. We reshape the tensor by combining the first two dimensions (D_F, T_{in}) and then perform temporal convolutions on the combined dimension with a softmax operation across the output modes dimension M as shown in Figure 4.

The total loss is shown in Eqn. 4. L_{ce} is the cross entropy loss from ranking the modes by their predicted probabilities. L_{reg}^{min} is the reconstruction loss for predicting the trajectories.

$$L = L_{ce} + L_{reg}^{min} \quad (4)$$

During training, we predict all M output modes. However, we only have one ground truth trajectory per agent, and thus use L_{reg}^{min} . Similar to the variety loss in [2] for penalizing multi-modal outputs, we penalize the minimum error mode L_{reg}^{min} out of all output modes to preserve multi-modality for all agents as shown in Eqn. 5. m_{min} is the minimum error mode, Y^k is the ground-truth future trajectory, and \hat{Y}_m^k is a

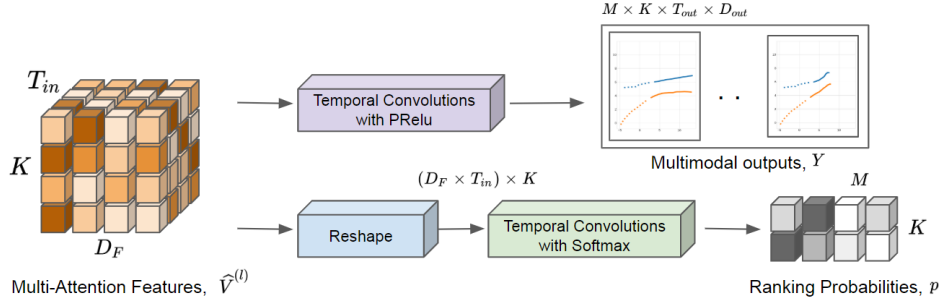


Fig. 4. Decoding multi modal trajectories and probabilities for each mode and agent

prediction mode (m) of agent k .

$$\begin{aligned}
 L_{reg}^{min} &= \sum_k L_{reg}(Y_{m_{min}}^k) \\
 m_{min} &= \arg \min_m L_{reg}(Y_m^k) \\
 L_{reg}(Y_m^k) &= \left\| Y^k - \hat{Y}_m^k \right\|_2
 \end{aligned} \quad (5)$$

Since there is no ground truth for probabilities associated with each mode, we penalize each mode in an unsupervised manner as shown in Eqn. 6, where $p_{gt}^{k,m}$ is the ground-truth probability and $p_{pred}^{k,m}$ is the prediction probability for mode m of agent k . $p_{gt}^{k,m}$ is generated using the minimum error criteria. We find the ground-truth probability of each prediction mode based on its proximity to the ground truth trajectory. Finally, ce is cross entropy for classification.

$$\begin{aligned}
 L_{ce} &= \sum_k \sum_m ce(p_{gt}^{k,m}, p_{pred}^{k,m}) \\
 p_{gt}^{k,m} &= \begin{cases} 1 & , m = m_{min} \\ 0 & , otherwise \end{cases}
 \end{aligned} \quad (6)$$

D. Evaluation Metrics

Evaluation of future trajectory is conducted by computing the Euclidean (L2) distance between the predicted and ground-truth locations. The standard error metrics are Average Displacement Error (ADE), Final Displacement Error (FDE) for single-modal prediction, and minimum Average Displacement Error (ADE_{min}), minimum Final Displacement Error (FDE_{min}) for multi-modal prediction with M output modes:

$$\begin{aligned}
 ADE &= \frac{1}{T_{out}} \sum_t \|x_t - \hat{x}_t\|_2 \\
 FDE &= \|x_T - \hat{x}_T\|_2 \\
 ADE_{min} &= \min_m ADE(m) \quad \forall m \in \{1, \dots, M\} \\
 FDE_{min} &= \min_m FDE(m) \quad \forall m \in \{1, \dots, M\}
 \end{aligned} \quad (7)$$

Although these metrics quantify the performance of prediction algorithms, the oracle use of such metrics to evaluate multi-modality has the following inherent limitations: (i) considering only one trajectory with the lowest error, these metrics compute the performance upper bound and simply overlook the diversity of multiple modes; and (ii) these

metrics do not take a prediction confidence into account if the associated probability were available. To address these limitations, we introduce new error metrics that can evaluate the diversity of multi-modal predictions with their associated confidence.

For any selected mode \hat{m} (using some criteria like mean or maximum probability), we find the error contributed by other modes $\mathcal{M} = E(e_i) - \hat{p} * \hat{e}$, excluding error \hat{e} contributed by probability \hat{p} of mode (\hat{m}) from expectation of all modes errors $E(e_i)$. Based on this, we introduce two new metrics that do not make any assumption on the method's output distribution: (i) The \mathcal{M}_1 metric is straightforward to compute the diversity of trajectories with respect to the ground-truth as we subtract the error contributed by the best mode (\hat{e}) from the expectation of errors of all modes by assigning equal probability ($1/M$) to all modes including the best mode ($\hat{p} = 1/M$). Therefore, we see how diverse the predicted samples are on average for the given test dataset. (ii) The \mathcal{M}_2 metric is designed to evaluate the error contribution of other modes with respect to their confidence. We subtract weighted error of the best mode ($\hat{e} = e_{p_{max}}$, maximum probability mode error with $\hat{p} = p_{max}$) from the weighted expectation of errors of all modes using the probabilities predicted. Therefore, we measure how distributed the predicted samples are with respect to their probability. With lower values, the prediction model is likely to be certain about its output with high accuracy.

$$\begin{aligned}
 \mathcal{M}_1 &= \frac{1}{M} \left(\left(\sum_i e_i \right) - \hat{e} \right) \\
 \mathcal{M}_2 &= \left(\sum_i p_i * e_i \right) - p_{max} * e_{p_{max}}
 \end{aligned} \quad (8)$$

We choose \hat{e} (best mode error) either as e_μ (error contributed by the mean of their output distribution) when the probabilities are not available [7] or as $e_{p_{max}}$ (error contributed by the p_{max} maximum probability mode) when the probabilities are associated with each mode like our Social-STAGE.

IV. EXPERIMENTAL RESULTS

We evaluate 5 different scenarios on publicly available ETH [28]-UCY [29] datasets that have been widely used in pedestrian trajectory forecast. We use the same splits of train, validation, and test sets as in [2], [7] for a fair comparison.

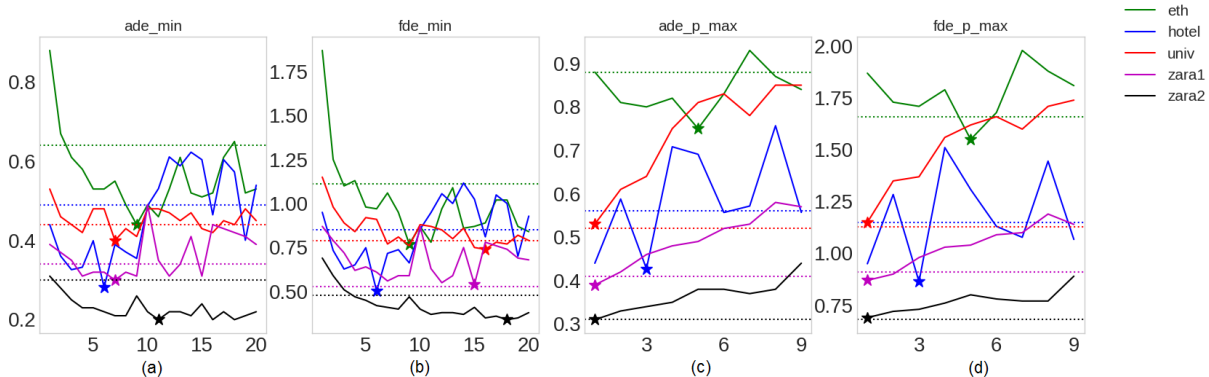


Fig. 5. Modes vs Metrics: We plot number of modes on x axis and different errors (in meters) on y-axis for all 5 different sets of ETH-UCY. The dotted line shows corresponding best state-of-the-art baseline in that set and metric. Star denotes to best number of modes to represent that dataset.

	ETH	Hotel	Univ	Zara1	Zara2	Avg
LSTM	1.09 / 2.41	0.86 / 1.91	0.61 / 1.31	0.41 / 0.88	0.52 / 1.11	0.70 / 1.52
S-LSTM [6]	1.09 / 2.35	0.79 / 1.76	0.67 / 1.40	0.47 / 1.00	0.56 / 1.17	0.72 / 1.54
S-Attn [3]	1.39 / 2.39	2.51 / 2.91	1.25 / 2.54	1.01 / 2.17	0.88 / 1.75	1.41 / 2.35
CIDNN [15]	1.25 / 2.32	1.31 / 2.36	0.90 / 1.86	0.50 / 1.04	0.51 / 1.07	0.89 / 1.73
SGAN [2]	1.13 / 2.21	1.01 / 2.18	0.60 / 1.28	0.42 / 0.91	0.52 / 1.11	0.74 / 1.54
S-STGCNN [7]	0.92 / 1.81	0.76 / 1.49	0.63 / 1.26	0.52 / 1.06	0.44 / 0.90	0.65 / 1.30
STGAT [27]	0.88 / 1.66	0.56 / 1.15	0.52 / 1.13	0.41 / 0.91	0.31 / 0.68	0.54 / 1.11
S-STAGE (ours-single)	0.88 / 1.87	0.44 / 0.95	0.53 / 1.15	0.39 / 0.87	0.31 / 0.69	0.51 / 1.11
Maximum Probability Mode Error ↓						
S-STAGE (ours-pmax) m_{pmax} : [5,3,1,1,1]	0.75 / 1.55	0.43 / 0.86	0.53 / 1.15	0.39 / 0.87	0.31 / 0.69	0.48 / 1.02

TABLE I
SINGLE-MODAL ADE / FDE FOR $T_{pred} = 12$ TIMESTEPS ARE REPORTED IN METERS.

	ETH	Hotel	Univ	Zara1	Zara2	Avg
SGAN-20 [2]	0.81 / 1.52	0.72 / 1.61	0.60 / 1.26	0.34 / 0.69	0.42 / 0.84	0.58 / 1.18
Sophie-30 [22]	0.70 / 1.43	0.76 / 1.67	0.54 / 1.24	0.30 / 0.63	0.38 / 0.78	0.54 / 1.15
Social-bigat-20 [13]	0.69 / 1.29	0.49 / 1.01	0.55 / 1.32	0.30 / 0.62	0.36 / 0.75	0.48 / 1.00
STGAT-20 [27]	0.65 / 1.12	0.35 / 0.66	0.52 / 1.10	0.34 / 0.69	0.29 / 0.60	0.43 / 0.83
S-STGCNN-20 [7]	0.64 / 1.11	0.49 / 0.85	0.44 / 0.79	0.34 / 0.53	0.30 / 0.48	0.44 / 0.75
S-STAGE (ours-multi) m_{min} : [9,6,7,7,11]	0.44 / 0.77	0.28 / 0.50	0.40 / 0.77	0.30 / 0.56	0.20 / 0.37	0.32 / 0.59

TABLE II
MULTI-MODAL ADE_{min} / FDE_{min} METRIC FOR $T_{pred} = 12$ TIMESTEPS ARE REPORTED IN METERS.

	ETH	Hotel	Univ	Zara1	Zara2	Avg
\mathcal{M}_1 -metric ↑						
S-STGCNN-20 [7]	1.00 / 1.79	0.77 / 1.44	0.71 / 1.35	0.62 / 1.16	0.54 / 1.01	0.73 / 1.35
S-STAGE (m_{pmax})	1.17 / 2.56	0.59 / 1.34	-	-	-	0.88 / 1.95
S-STAGE (m_{min})	1.63 / 3.44	0.75 / 1.74	1.05 / 2.31	1.09 / 2.45	1.17 / 2.47	1.14 / 2.48
\mathcal{M}_2 -metric ↓						
S-STAGE (m_{pmax})	0.07 / 0.16	0.15 / 0.33	-	-	-	0.11 / 0.24
S-STAGE (m_{min})	0.06 / 0.14	0.03 / 0.06	0.17 / 0.34	0.08 / 0.16	0.13 / 0.26	0.09 / 0.19

TABLE III
 \mathcal{M}_1 AND \mathcal{M}_2 ASSOCIATED WITH ADE / FDE FOR $T_{pred} = 12$ TIMESTEPS ARE REPORTED IN METERS.

A. Quantitative results

In Table I, II, III, we show different types of quantitative evaluations of our framework on ETH-UCY datasets by comparing to other state-of-the-art baselines. Errors of all baselines and our Social-STAGE (S-STAGE for simplicity)

are reported in meters, with 8 time steps of observations and 12 time steps of predictions in future. In Table I, we show single-modal comparisons. Our S-STAGE (single-modal) with graph convolution module and multi-attention outperforms similar graph-based methods such as S-STGCNN [7]

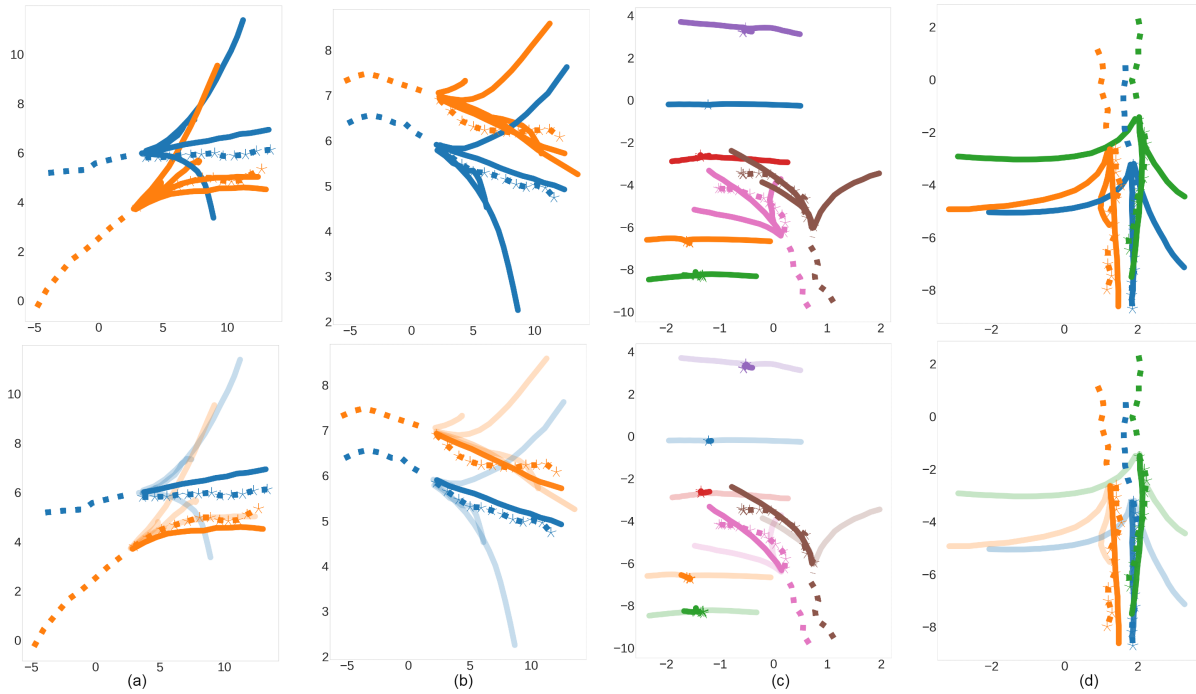


Fig. 6. Social-STAGE qualitative results. Different agents are shown in different colors. First row all modes with equal probability. Second row with probability as opacity. Columns (a,b) from ETH test-set, and columns (c,d) from hotel test-set.

and STGAT [27]. Note that single modal comparisons are not reported in the S-STGCNN paper. Therefore, our evaluation is based on their publicly available trained models and code. We use the mean from the Gaussian prediction for S-STGCNN single-modal evaluation baseline. We additionally report S-STAGE (ours p_{max}) that is using the best mode of trajectory (with the highest probability) for evaluation. This model performs better overall comparing to all other baselines. It highlights the efficacy of our ranking capability. We also report the best number of modes that are empirically calculated as shown in Figure 5. Here, we plot the metrics on Y-axis and modes on X-axis with corresponding best baseline in dashed line. We observe that p_{max} error does not decrease with more number of modes in Figure 5 (c-d). The best performance is shown from 5 modes for ETH and 3 modes for Hotel. However, in case of Univ, Zara1, Zara2, the maximum probability error $m_{p_{max}} = 1$ is the same as those of S-STAGE (ours-single), which seems consistent with the motion complexity of these sets.

For multi-modal comparison, the best performing modes for ADE is different with those of FDE as shown in Figure 5 (a-b). We choose best number of modes (m_{min}) based on minimum ADE_{min} for reporting both ADE_{min} and FDE_{min} . The minimum error metrics are shown in Table II for multi-modal prediction. Interestingly, we observe that S-STAGE performs the best even with less number of modes in all sets compared to the baseline models, which demonstrate the robustness of the proposed framework.

We also report our new metrics \mathcal{M}_1 and \mathcal{M}_2 in Table III to evaluate diversity of different modes (\mathcal{M}_1) and with their confidence (\mathcal{M}_2). For \mathcal{M}_1 , we compare with S-STGCNN-20 using $\hat{e} = e_\mu$ as their best mode error. We observe in \mathcal{M}_1 that

the model trained for the maximum probability mode, $m_{p_{max}}$ (with 5 modes for ETH), achieves better diversity than 20 modes sampled from S-STGCNN. When we compare our m_{min} ([9,6,7,7,11]) model that is trained for multi-modal evaluation for this metric, it shows the way higher diversity among the predicted trajectories. For evaluation on \mathcal{M}_2 , note that we compare our $m_{p_{max}}$ and m_{min} modes baselines since the compared state-of-the-art methods do not provide probabilities associated with prediction samples. We observe that both baselines perform similar in the ETH set. But for the Hotel set, we find more modes are giving less error. Overall, we find that the m_{min} baseline predicts high confident probabilities.

B. Qualitative results

We show qualitative results of our model for both multi-modal predictions and ranking in Figure 6. Different pedestrians are visualized using different colors. Top row shows multi-modal prediction scenarios (a,b) from ETH set (with number of modes $M = 5$) and (c,d) from hotel set (with number of modes $M = 3$). In scenario (a,b), when two pedestrians walk closely, the predictions are made with max probability close to ground truth based on the motion cues and interaction cues. In scenario (c), there are many pedestrians standing and not moving. Based on their motion cues, the predicted max probability mode generates 'standing' in the future. Also, other modes predict that they can move in two opposite directions, which demonstrates the diversity of our proposed model. In the same scenario (c), there are two pedestrians walking beside each other. Based on motion cues, the network predicted that turning left trajectory as a dominant mode. In scenario (d), three pedestrians are

walking very closely along side of each other. Our model predicts going straight as a more dominant future, but at the same time, we also predict other possibilities of turning left or right, which is common and plausible in real scenarios.

V. IMPLEMENTATION AND MODEL DETAILS

We provide details of our model implementation below with the following settings: an example batch size of 1; number of agents $K=4$; number of output modes $M=2$; number of input time steps $T_{in}=8$; and number of output time steps $T_{out}=12$. We trained for 100 epochs with M ranging from 0 to 20. We reported best epoch and best modes M results. We used a learning rate of 0.0001 and trained our model on Quadro RTX 6000 GPU. We used the PyTorch framework for the implementation.

	Layer	Kernal shape	Output shape
Graph Convolutions			
0	l1.BatchNorm2d	[2]	[1, 2, 8, 4]
1	l1.PReLU	[1]	[1, 2, 8, 4]
2	l1.Conv2d	[2, 2, 3, 1]	[1, 2, 8, 4]
3	l1.BatchNorm2d	[2]	[1, 2, 8, 4]
4	l1.Dropout	-	[1, 2, 8, 4]
5	l2.Conv2d	[2, 2, 1, 1]	[1, 2, 8, 4]
6	l2.PReLU	[1]	[1, 2, 8, 4]
7	graph conv update using adjacency matrix, follow Equation [2] from manuscript		
Attention Module			
8	attn.BatchNorm2d	[2]	[1, 2, 8, 4]
9	attn.PReLU	[1]	[1, 2, 8, 4]
10	attn.Conv2d	[2, 2, 3, 1]	[1, 2, 8, 4]
11	attn.BatchNorm2d	[2]	[1, 2, 8, 4]
12	attn.Softmax	-	[1, 2, 8, 4]
13	using attn weights from step 12, follow Equation [3] from manuscript (multi-attention operation)		
Decoder			
14(a)	d.Conv2d	[8, 24, 3, 3]	[1, 24, 2, 4]
15(a)	d.PReLU	[1]	[1, 24, 2, 4]
16(a)	traj.Conv2d	[24, 24, 3, 3]	[1, 24, 2, 4]
16(b)	prob.Conv2d	[16, 2, 3, 3]	[1, 2, 1, 4]
17(a)	traj.reshape	-	[1, 2, 12, 2, 4]

TABLE IV
S-STAGE MODEL SUMMARY

D_{in} is the input dimension of the trajectory at each time step, since the ETH-UCY dataset consists of 2D motion of pedestrians $D_{in} = 2$. D_{out} is the output dimension of the trajectory, if the prediction is Gaussian distribution for each mode (gaussian mixture) D_{out} should be 5 (containing variance and correlation outputs), if the prediction is a direct trajectory regression D_{out} should be 2. We present $D_{out} = 2$ in this work, as we observed $D_{out} = 5$ with negative log-likelihood for multi-modal setup did-not perform better than $D_{out} = 2$ with rmse as a common issue of mode collapse while training mixture distributions [19,20,21,8,9,4].

VI. CONCLUSION

We presented a trajectory prediction framework that aims to generate plausible future trajectories with a diversity, considering spatio-temporal interactions of agents. Given the

agents' motion history, we explored the spatial influences of individual agents and their temporal changes. We then found the relative importance of interactions using multi-attention, which can be simultaneously captured along the spatial and temporal dimension. The resulting features were used to generate multiple future trajectories with corresponding probabilities to rank each mode. To this end, we evaluated our approach using the public benchmark datasets and showed significant improvement for single- and multi-modal prediction on the standard ADE and FDE metrics as well as \mathcal{M}_1 and \mathcal{M}_2 that were newly introduced in this work to evaluate the diversity with associated probability of multi-modal prediction.

REFERENCES

- [1] N. Lee, W. Choi, P. Vernaza, C. B. Choy, P. H. Torr, and M. Chandraker, "Desire: Distant future prediction in dynamic scenes with interacting agents," in *Proceedings of the IEEE Conference on Computer Vision and Pattern Recognition*, 2017, pp. 336–345.
- [2] A. Gupta, J. Johnson, L. Fei-Fei, S. Savarese, and A. Alahi, "Social gan: Socially acceptable trajectories with generative adversarial networks," in *Proceedings of the IEEE Conference on Computer Vision and Pattern Recognition*, 2018, pp. 2255–2264.
- [3] A. Vemula, K. Muelling, and J. Oh, "Social attention: Modeling attention in human crowds," in *2018 IEEE International Conference on Robotics and Automation (ICRA)*. IEEE, 2018, pp. 1–7.
- [4] H. Cui, V. Radosavljevic, F.-C. Chou, T.-H. Lin, T. Nguyen, T.-K. Huang, J. Schneider, and N. Djuric, "Multimodal trajectory predictions for autonomous driving using deep convolutional networks," in *2019 International Conference on Robotics and Automation (ICRA)*. IEEE, 2019, pp. 2090–2096.
- [5] S. Malla, B. Dariush, and C. Choi, "Titan: Future forecast using action priors," in *Proceedings of the IEEE/CVF Conference on Computer Vision and Pattern Recognition*, 2020, pp. 11 186–11 196.
- [6] A. Alahi, K. Goel, V. Ramanathan, A. Robicquet, L. Fei-Fei, and S. Savarese, "Social lstm: Human trajectory prediction in crowded spaces," in *Proceedings of the IEEE conference on computer vision and pattern recognition*, 2016, pp. 961–971.
- [7] A. Mohamed, K. Qian, M. Elhoseiny, and C. Claudel, "Social-stgcn: A social spatio-temporal graph convolutional neural network for human trajectory prediction," in *Proceedings of the IEEE/CVF Conference on Computer Vision and Pattern Recognition*, 2020, pp. 14 424–14 432.
- [8] J. Curro and J. Raquet, "Deriving confidence from artificial neural networks for navigation," in *2018 IEEE/ION Position, Location and Navigation Symposium (PLANS)*. IEEE, 2018, pp. 1351–1361.
- [9] S. Messaoud, D. Forsyth, and A. G. Schwing, "Structural consistency and controllability for diverse colorization," in *Proceedings of the European Conference on Computer Vision (ECCV)*, 2018, pp. 596–612.
- [10] O. Makansi, E. Ilg, O. Cicek, and T. Brox, "Overcoming limitations of mixture density networks: A sampling and fitting framework for multimodal future prediction," in *Proceedings of the IEEE Conference on Computer Vision and Pattern Recognition*, 2019, pp. 7144–7153.
- [11] C. Choi, A. Patil, and S. Malla, "Drogon: A causal reasoning framework for future trajectory forecast," *arXiv preprint arXiv:1908.00024*, 2019.
- [12] C. Choi, "Shared cross-modal trajectory prediction for autonomous driving," *arXiv preprint arXiv:2004.00202*, 2020.
- [13] V. Kosaraju, A. Sadeghian, R. Martín-Martín, I. Reid, H. Rezatofighi, and S. Savarese, "Social-bigat: Multimodal trajectory forecasting using bicycle-gan and graph attention networks," in *Advances in Neural Information Processing Systems*, 2019, pp. 137–146.
- [14] S. Yan, Y. Xiong, and D. Lin, "Spatial temporal graph convolutional networks for skeleton-based action recognition," in *Thirty-second AAAI conference on artificial intelligence*, 2018.
- [15] Y. Xu, Z. Piao, and S. Gao, "Encoding crowd interaction with deep neural network for pedestrian trajectory prediction," in *Proceedings of the IEEE Conference on Computer Vision and Pattern Recognition*, 2018, pp. 5275–5284.

- [16] P. Zhang, W. Ouyang, P. Zhang, J. Xue, and N. Zheng, "Sr-lstm: State refinement for lstm towards pedestrian trajectory prediction," in *Proceedings of the IEEE Conference on Computer Vision and Pattern Recognition*, 2019, pp. 12 085–12 094.
- [17] Y. Ma, X. Zhu, S. Zhang, R. Yang, W. Wang, and D. Manocha, "Trafficpredict: Trajectory prediction for heterogeneous traffic-agents," in *Proceedings of the AAAI Conference on Artificial Intelligence*, vol. 33, 2019, pp. 6120–6127.
- [18] T. N. Kipf and M. Welling, "Semi-supervised classification with graph convolutional networks," *arXiv preprint arXiv:1609.02907*, 2016.
- [19] L. U. Hjorth and I. T. Nabney, "Regularisation of mixture density networks," in *1999 Ninth International Conference on Artificial Neural Networks ICANN 99.(Conf. Publ. No. 470)*, vol. 2. IET, 1999, pp. 521–526.
- [20] A. Graves, "Generating sequences with recurrent neural networks," *arXiv preprint arXiv:1308.0850*, 2013.
- [21] C. Rupprecht, I. Laina, R. DiPietro, M. Baust, F. Tombari, N. Navab, and G. D. Hager, "Learning in an uncertain world: Representing ambiguity through multiple hypotheses," in *Proceedings of the IEEE International Conference on Computer Vision*, 2017, pp. 3591–3600.
- [22] A. Sadeghian, V. Kosaraju, A. Sadeghian, N. Hirose, H. Rezafooghi, and S. Savarese, "Sophie: An attentive gan for predicting paths compliant to social and physical constraints," in *Proceedings of the IEEE Conference on Computer Vision and Pattern Recognition*, 2019, pp. 1349–1358.
- [23] Y. Chai, B. Sapp, M. Bansal, and D. Anguelov, "Multipath: Multiple probabilistic anchor trajectory hypotheses for behavior prediction," in *Conference on Robot Learning*, 2020, pp. 86–99.
- [24] B. Ivanovic and M. Pavone, "The trajectron: Probabilistic multi-agent trajectory modeling with dynamic spatiotemporal graphs," in *Proceedings of the IEEE International Conference on Computer Vision*, 2019, pp. 2375–2384.
- [25] L. A. Thiede and P. P. Brahma, "Analyzing the variety loss in the context of probabilistic trajectory prediction," in *Proceedings of the IEEE International Conference on Computer Vision*, 2019, pp. 9954–9963.
- [26] A. Vaswani, N. Shazeer, N. Parmar, J. Uszkoreit, L. Jones, A. N. Gomez, Ł. Kaiser, and I. Polosukhin, "Attention is all you need," in *Advances in neural information processing systems*, 2017, pp. 5998–6008.
- [27] Y. Huang, H. Bi, Z. Li, T. Mao, and Z. Wang, "Stgat: Modeling spatial-temporal interactions for human trajectory prediction," in *Proceedings of the IEEE International Conference on Computer Vision*, 2019, pp. 6272–6281.
- [28] S. Pellegrini, A. Ess, K. Schindler, and L. Van Gool, "You'll never walk alone: Modeling social behavior for multi-target tracking," in *2009 IEEE 12th International Conference on Computer Vision*. IEEE, 2009, pp. 261–268.
- [29] A. Lerner, Y. Chrysanthou, and D. Lischinski, "Crowds by example," in *Computer graphics forum*, vol. 26, no. 3. Wiley Online Library, 2007, pp. 655–664.